Geophysical Journal International

Geophys. J. Int. (2011) **187,** 1019–1026 doi: 10.1111/j.1365-246X.2011.05216.x

Receiver function images of the base of the lithosphere in the Alboran Sea region

Süleyman Dündar,[1] Rainer Kind,[1,2] Xiaohui Yuan,[1] Fatih Bulut,[1] Forough Sodoudi,[1,2] Ben Heit,[1] Prakash Kumar,[1,3] Xueqing Li,[1] Winfried Hanka,[1] Rosa Martin,[4] Manfred Stiller,[1] Tuna Eken,[1] Marcelo Bianchi,[1] Elisa Buforn[5] and Jose Martin Davila[6]

[1] *Deutsches GeoForschungsZentrum GFZ, Potsdam, Germany. E-mail: kind@gfz-potsdam.de*
[2] *Institut für Geologische Wissenschaften, Freie Universität, Berlin, Germany*
[3] *National Geophysical Research Institute NGRI, Hyderabad, India*
[4] *Instituto Andaluz de Geofisica, Granada IAG, Spain*
[5] *Universidad Complutense de Madrid UCM, Spain*
[6] *Real Observatorio de la Armada, San Fernando ROA, Spain*

Accepted 2011 August 17. Received 2011 August 17; in original form 2011 February 23

SUMMARY

We analyse data from seismic stations surrounding the Alboran Sea between Spain and North Africa to constrain variations of the lithosphere–asthenosphere boundary (LAB) in the region. The technique used is the receiver function technique, which uses *S*-to-*P* converted teleseismic waves at the LAB below the seismic stations. We confirm previous data suggesting a shallow (60–90 km) LAB beneath the Iberian Peninsula and we observe a similarly shallow LAB beneath the Alboran Sea where the lithosphere becomes progressively thinner towards the east. A deeper LAB (90–100 km) is observed beneath the Betics, the south of Portugal and Morocco. The structure of the LAB in the entire region does not seem to show any indication of subduction related features. We also observe good *P* receiver function signals from the seismic discontinuities at 410 and 660 km depth which do not indicate any upper-mantle anomaly beneath the entire region. This is in agreement with the sparse seismic activity in the mantle transition zone suggesting the presence of only weak and regionally confined anomalies.

Key words: Coda waves; Continental margins: convergent; Dynamics of lithosphere and mantle.

INTRODUCTION

The Alboran Sea region is located at the western end of the Mediterranean Sea and represents a part of the collision zone between the African and the Eurasian plates. Several models have been suggested to explain the different tectonic features in this region, but a generally agreed model does not exist yet. For example, GPS data tracking tectonic displacements in this region have been obtained and modelled by several authors (McClusky *et al*. 2003; Fadil *et al*. 2006; Perouse *et al*. 2010; Vernant *et al*. 2010). Vernant *et al*. (2010) used more than 40 permanent and temporary stations in Morocco and southern Spain. They suggest that the kinematic displacement of the region is associated with slab rollback towards the SSW and backarc opening in the Alboran Basin, superimposed on the Eurasia–Nubia differential motion. Other dynamic models also suggest subduction rollback for this region although in a more westerly direction, connected to the opening of the Alboran Basin (Morley 1993; Royden 1993; Lonergan & White 1997; Michard *et al*. 2002). Such models are supported by tomographic studies (e.g. Gutscher *et al*. 2002; Spakman & Wortel 2004). They found an east-dipping high-velocity slab beneath the Alboran Sea, reaching down to the mantle transition zone. However, Morales *et al*. (1999) suggested, also from a tomography study, a southward-directed subduction beneath the Betic mountains. Another suggested dynamical model for this region is the delamination of a deep portion of the lithospheric roots from an early collisional Betic–Rif orogen (Platt & Vissers 1989; Comas *et al*. 1992; Garcia-Duenas *et al*. 1992; Docherty & Banda 1995; Houseman 1996; Seber *et al*. 1996; Calvert *et al*. 2000). Such a model may require radially symmetric deformation which would be inconsistent with southward motion of both, the Betic and Rif mountains, as is suggested by Vernant *et al*. (2010). Buontempo *et al*. (2008) and Diaz *et al*. (2010) observe rotation of the fast split direction of *SKS* anisotropy following the curvature of the Betics and the Gibraltar Arc. In the interpretation of their observations, they favour the slab rollback model rather than the delamination model.

The crustal thickness beneath the Iberian Peninsula and surrounding areas has been recompiled by Diaz & Gallart (2009) from different controlled source seismic experiments. High-resolution crustal structure was obtained from the IBERSEIS project in 2001 in

© 2011 The Authors
Geophysical Journal International © 2011 RAS

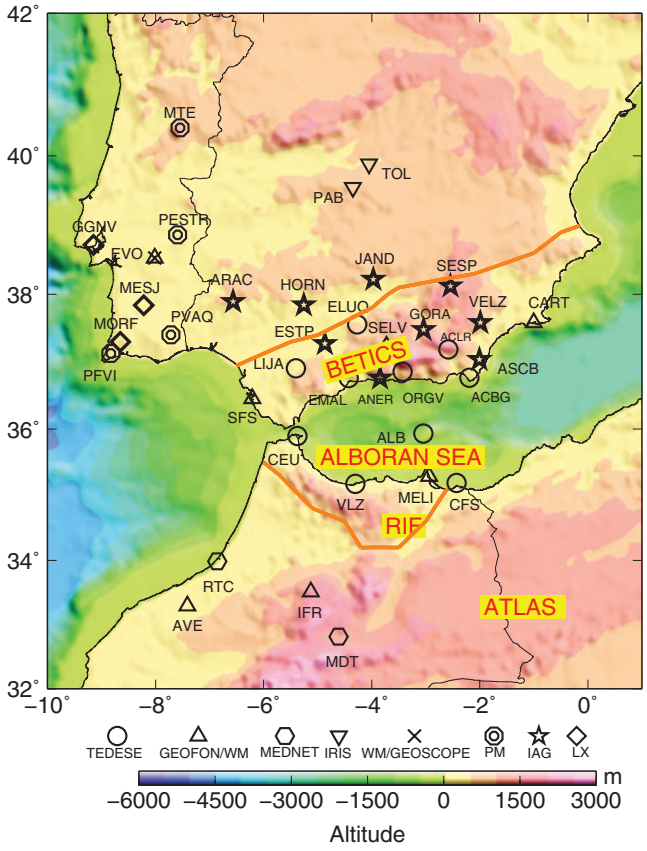

Figure 1. Map of the seismic broad-band stations used: TEDESE, temporary network 2001–2004 of UCM, ROA and GEOFON (Buforn *et al*. 2002); PM, Portuguese National Seismic Network; IAG, Network of Instituto Andaluz de Geofísica, Granada; LX, University of Lisbon Seismic Network.

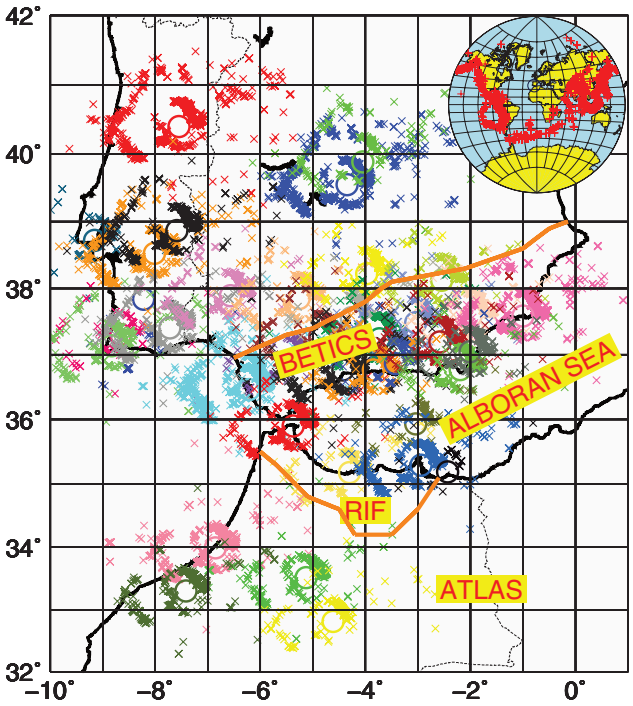

Figure 2. Piercing points (sites of *S*-to-*P* conversion) of *S* and *SKS* phases at 100 km depth for the earthquake records used in this study. *SKS* piercing points are closer to the stations than *S* piercing points due to their steeper incidence angles. Station locations are marked by circles with the same colour as the according piercing points (crosses). For some areas, we have a very dense coverage of piercing points (especially in the Betics) since the spacing between stations is very small. The Alboran Sea, even with the lack of stations, is also relatively well covered with piercing points due to the large offset of *S*-to-*P* conversion points from the stations. The inset on the top right shows the distribution of teleseismic events used for *S* and *SKS* epicentral distances (red crosses).

southwest Iberia (Simancas *et al*. 2003; Carbonell *et al*. 2004). The Moho depth is near 30 km beneath the central parts of Iberia, it reaches about 38 km beneath the Betics in southern Spain and shallows beneath the Alboran Sea to about 15 km. In Morocco, north of the High Atlas, Wigger *et al*. (1992) found the Moho at a depth of 35 km. This depth was confirmed with receiver functions by Sandvol *et al*. (1998). Fullea *et al*. (2007, 2009) modelled the LAB depth around the Alboran Sea from elevation, geoid and thermal data and obtained 140–160 km beneath the Betics and Gibraltar and about 100 km beneath the eastern Alboran Sea. Palomeras *et al*. (2010) obtained in southwest Iberia LAB depths of 95–120 km based on the results of Fullea *et al*. (2007) and of detailed crustal models from IBERSEIS.

Obvious effects of the plate collision are the relatively sparse earthquakes occurring in this region, which do not mark the Eurasian–African plate boundary very clearly (e.g. Buforn *et al*. 2004). There are shallow and deep seismic events of low to moderate magnitude with some strong destructive earthquakes in historical times. Some of these earthquakes reached maximum intensities of *X* on the Mercalli scale, such as the Torrevieja 1829 and Arenas del Rey 1884 earthquakes (Muñoz & Udías, 1988). The most prominent earthquake that took place in this region is the Lisbon event from 1755 that originated in the Gulf of Cadiz in the Atlantic Ocean with a magnitude estimated to be about 8.5 (e.g. Martinez-Solares & López Arroyo 2004; Zitellini *et al*. 2009). The distribution of earthquake hypocentres is relatively unclear, with some events reaching depths of about 650 km (e.g. Buforn *et al*. 1997).

METHOD AND DATA

The aim of this study is to image the depth distribution of the lithosphere–asthenosphere boundary (LAB) in the Alboran Sea region. Knowledge about the geometry of this discontinuity may be even more helpful for understanding the collision process than knowledge of the crustal structure. The *S* receiver function technique (e.g. Yuan *et al*. 2006) is able to provide detailed information about the depth distribution of the LAB. It should also be mentioned that *S* receiver functions have the advantage of being free from multiples, unlike *P* receiver functions, which excludes misinterpretations of the LAB signals as multiples. This technique is now frequently used in many parts of the world (see the review by Fischer *et al*. 2010 and references therein). It identifies seismic phases, which are converted from *S*-to-*P* at the LAB under each station. These signals are precursors of the *S* phase of teleseismic events. The teleseismic data used in this study originate from seismic broad-band stations operated by different institutions. The location of the 38 stations used and the operating institutions are marked in Fig. 1. Fig. 2 shows the distribution of the *S*-to-*P* conversion points at a reference depth of 100 km using all available seismic records. We analysed about 14 000 *S* receiver functions. Fig. 3 shows summed *S* and *SKS* receiver functions for each

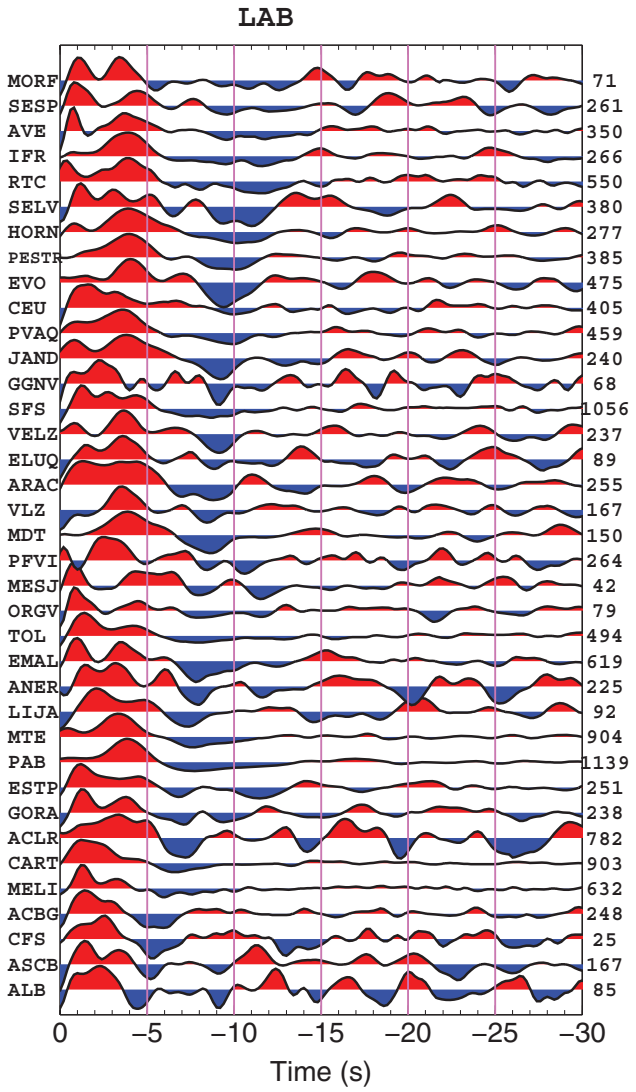

Figure 3. Summed *S* receiver functions for each station to demonstrate the data quality. Displayed is the *P* component (also called *L* component) that is obtained by rotating the original radial and vertical components into the ray coordinate system *P* and *SV*. This system approximately separates *P* and *SV* energy. Zero time is the arrival time of the *S* phase on the *SV* component (also called *Q* component). The numbers on the right are the number of seismic traces summed for each station. The positive (red) and negative (blue) signals originate from discontinuities with velocity increase and decrease downward, respectively. The red signals between 0 and –5 s originate from conversions at the Moho and internal crustal discontinuities. The blue signals from –5 to –15 s indicate a low-velocity zone below the Moho (interpreted as lithosphere–asthenosphere boundary, LAB). The traces are sorted according to increasing LAB times. This figure demonstrates clearly that the blue signal is not a side lobe of the Moho, otherwise both signals would be parallel. For a geographical distribution of the receiver functions, see Figs 4, 6 and 7.

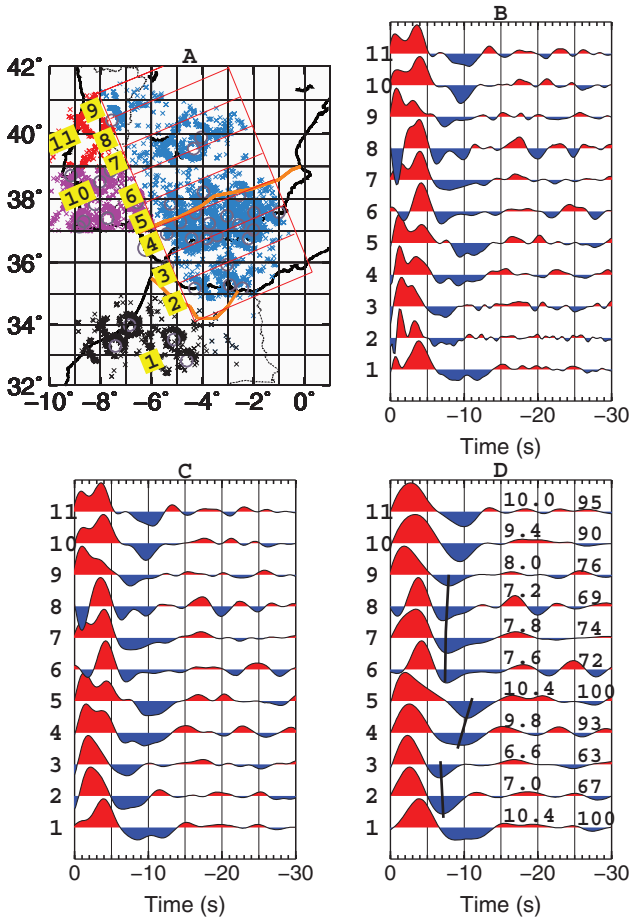

Figure 4. (a) Boxes 1–11 denote piercing point regions defined for summation of the according seismic traces. Region 1 is in North Africa, regions 2–9 are oriented along a 200 km broad profile perpendicular to the Betic mountains and regions 10 and 11 cover mainly southern Portugal. Parts (b), (c) and (d) show summation traces of *S* and *SKS* precursors in each defined region for different bandpass filters [(b): 1–30 s, (c): 3–30 s, (d): 5–30 s]. Black lines in (d) mark the deepening LAB from the Alboran Sea to north of the Betic mountains (regions 2–5) and the again shallower LAB in the north of the profile (6–9). The LAB in northern Africa (region 1) shows a double LAB phase partly consistent with the Betics and partly consistent with the Alboran Sea. This could be due to the very different tectonic environment sampled by this area, ranging from the west coast of Africa to the Atlas mountains. Southern Portugal (regions 10 and 11) has about the same LAB depth as in the Betic mountains. The numbers indicated on the traces in (d) are the averaged precursor times in seconds and depths of the LAB in kilometres in each box. It should be noted that traces 1, 10 and 11 are not located along the profile perpendicular to the Betics.

station. That means all traces recorded at one station are stacked after rotation, deconvolution, normalization and distance (or slowness) moveout correction. A reference slowness of 6.4 s deg^{-1} was used for the moveout correction. This value is frequently used for *P* receiver functions. We used the same value for the *S* receiver functions to obtain comparable time differences. Two groups of signals are easily recognized. The first group arrives about 5 s or less before the *S* onset. This group originates from the interior of the crust and from the Moho. Nearly all these signals are positive which means they are caused by a velocity increase downward. The second group of signals arrives between 4 and 15 s before the *S* onset. This group is predominantly negative which means that the signals are caused by *S*-to-*P* conversions at a discontinuity with downward decreasing velocity below the Moho. In this case, this signal group is indicating the existence of a seismic low-velocity zone beneath each one of the stations. Traditionally, a seismic low-velocity zone in the upper mantle is assumed to be the asthenosphere. Therefore, we interpret the negative signal in *S* receiver functions as caused by the upper boundary of the asthenosphere, the LAB.

The receiver functions in Fig. 3 are time-series and the precursor times of the LAB signals must be converted into depth using a

© 2011 The Authors, *GJI*, **187,** 1019–1026
Geophysical Journal International © 2011 RAS

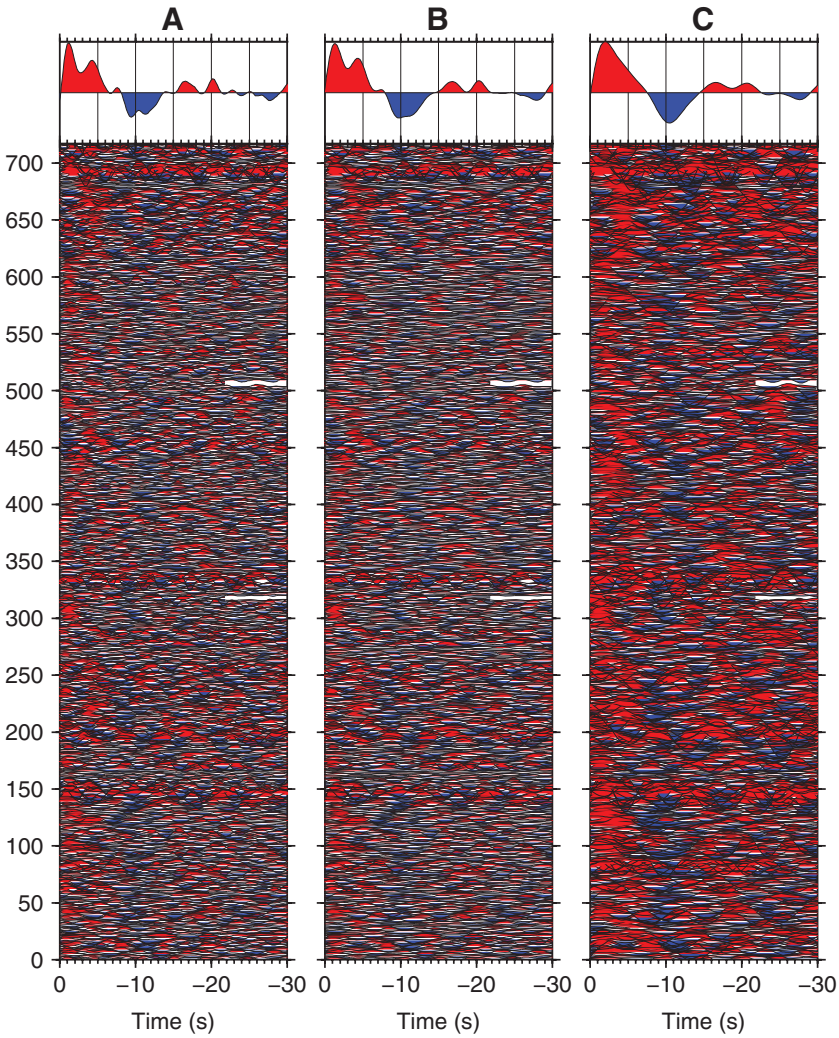

Figure 5. Individual *S* receiver function traces (below) and summation traces (top) for region number 5 in Fig. 4. Panels (a), (b) and (c) correspond to 1–30 s, 3–30 s and 5–30 s bandpass filters, respectively. Traces are moveout corrected for a reference slowness of 6.4 s deg^{-1}. More than 700 traces have been summed for this region. Different filters are used to demonstrate the stability of the observations.

velocity model. If we use the global reference model IASP91 (Kennett & Engdahl 1991), we obtain depth estimates from LAB times by multiplying those by a factor of about 9.5. For more accurate depths determinations, local velocity models should be used.

Station summations, like in Fig. 3, are good for checking the data quality. However, to obtain information from a discontinuity at a certain depth, it is more useful to sum traces which have neighbouring conversion points. Therefore, we define boxes including the neighbouring piercing points at 100 km depth and stack all traces with piercing points in one box. We selected relatively large boxes which can be seen in Fig. 4(a). The boxes are larger than the Fresnel zones and determine therefore the spatial resolution. Selecting boxes with smaller sizes increases the spatial resolution on the expenses of the number of traces in each box, which leads to reduced signal-to-noise ratio. We obtained only an average value for each box; within one box we have no resolution. No overlapping is applied; the values of each box are completely independent of each other. To illustrate the summation technique, we have shown in Fig. 5 for box 5 all individual seismic traces and the summation trace for three different bandpass filters.

RESULTS AND DISCUSSION

The boxes in Fig. 4 are selected to display a profile perpendicular to the Alboran Sea and the strike of the Betic mountains. The Alboran Sea (boxes 2 and 3) and the area north of the Betics (boxes 6–9) are the regions with the shallowest detected LAB depths (about 60–90 km). The LAB depths in the other boxes range from about 90–100 km (Africa, box 1; the Betics and just north of it, boxes 4–5 and southern Portugal, boxes 10–11).

Fig. 6 shows a profile across the Alboran Sea from the west to the east. The LAB is deep (near 90 km) in the Atlantic near the southern part of Portugal and shallowing from there in easterly direction across the Alboran Sea to about 60 km (especially clear in the long-period version, see Fig. 6(d)). Also the Moho seems to be shallowing to the east in the Alboran Sea. More detailed images than from *S* receiver functions about the Moho may be obtained from *P* receiver functions. However, the station density should be higher for a complete *P* receiver function image. Ocean bottom stations would be required to cover the Alboran Sea and should help to constrain the depth variations in a more reliable way.

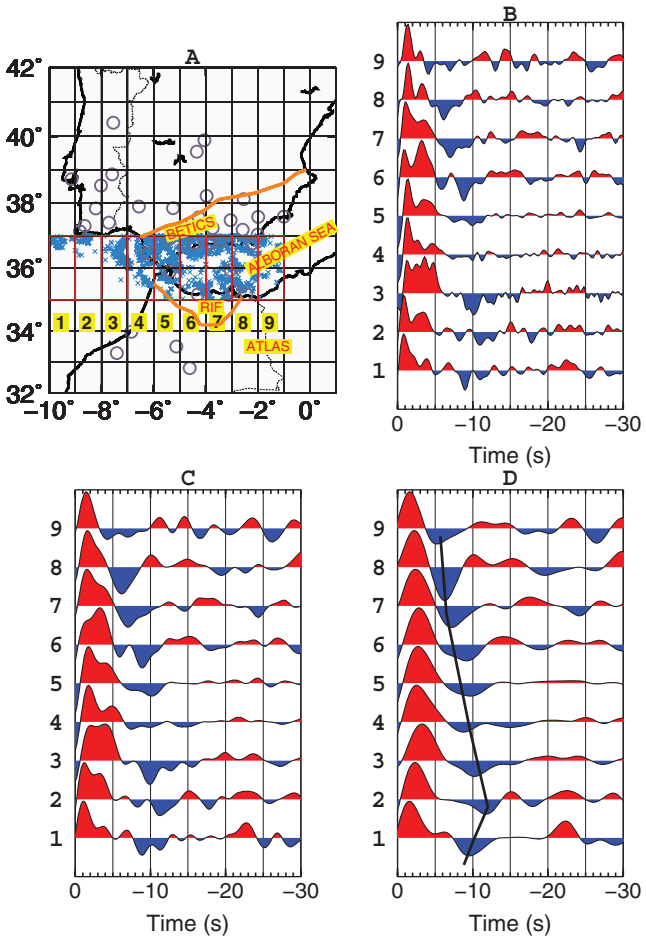

Figure 6. As in Fig. 4, for a profile from the west of Gibraltar to the east across the Alboran Sea. The black line in (d) indicates shallowing of the LAB from Gibraltar to the east from about 100 to 60 km. Seismic stations positions are marked by circles in the map.

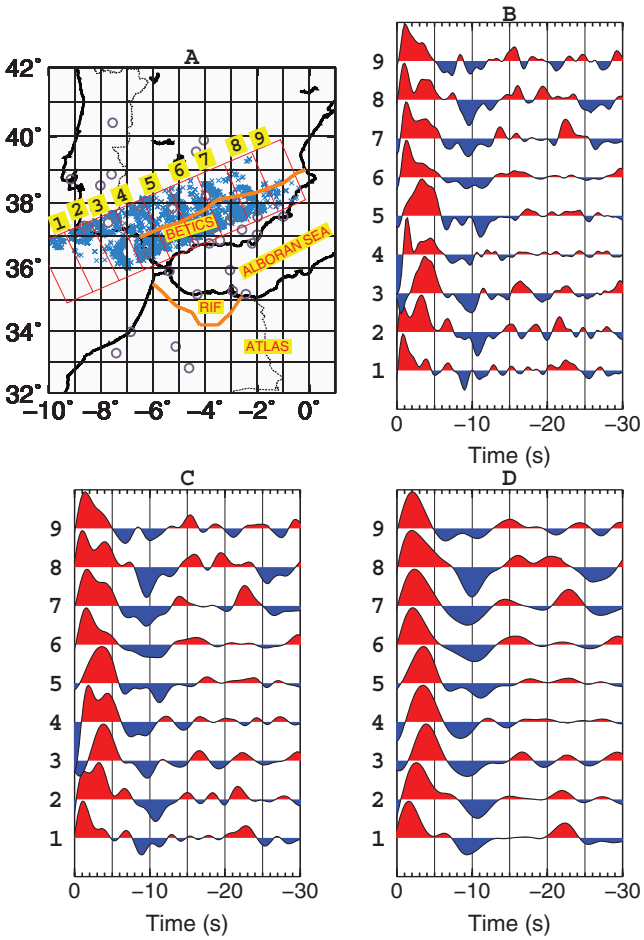

Figure 7. Same as in Fig. 4 for a profile along the strike of the Betic Mountains. The LAB depth remains, with some scatter, relatively constant along the entire profile.

By constructing a profile along strike of the Betics (Fig. 7), we see that there are much less changes than in Fig. 6 across the Alboran Sea. The LAB phases in the Betics remain at similar delay times around 10 s (Fig. 7). There is also a clear difference between the LAB structure along the strike of the Betics (Fig. 7) and the one perpendicular to the strike of the Betics (Fig. 4). There is much more LAB topography perpendicular to the strike of the Betics (Fig. 4).

We have produced a map of the LAB (see Fig. 8(a)) in the region of the Alboran Sea, which displays averaged values for the different tectonic units. Details can be seen along the individual profiles (see Figs 4, 6 and 7). A large part of Iberia, north of the Betics, shows a shallow LAB (less than 90 km depth). These results are in good agreement with surface wave observations of a low-velocity zone below about 80 km in the entire region north of the Betics (Martinez *et al*. 2005). Ayarza *et al*. (2010), however, have found a signal from 60–70 km depth in wide-angle reflection data in southwest Iberia and have modelled it with a velocity increase and interpreted it as the Hales discontinuity. The question, however, if a high-frequency wide-angle reflection from the upper mantle is caused by a velocity increase or decrease, is usually difficult to answer. It depends strongly on the identification of the sign of the reflected signal. Such a reflection should have a positive sign in case of a velocity increase and a negative sign in case of a decrease. Ayarza *et al*. (2010) have not shown clear evidence that their mantle reflection has a positive sign. In our opinion, a negative sign is equally possible. With such an interpretation, their result would agree very well with our data and the wide-angle reflection could have been caused by the LAB instead of the Hales discontinuity (which is usually thought to be positive). *S* receiver function data have usually no problem with the sign of the converted phases since they have much longer periods.

The Alboran Sea also has a shallow LAB, which is shallowest at its eastern part (see Fig. 6). Seber *et al*. (1996) and Houseman (1996) suggest the delamination model for the Alboran Sea, which is directly related to crustal and lithospheric thinning. Gutiérrez-Alonso *et al*. (2011) and Ducea (2011) suggest large-scale delamination below the Iberian Massif and replacement of the mantle lithosphere. This model is in good agreement with our observation of a thin lithosphere north of the Betics. This means there that are two regions in the western Mediterranean area where delamination is suggested and where we observed thinning of the lithosphere.

Southern Portugal, Gibraltar, the westernmost part of the Atlantic, the Betics and North Africa show a deeper LAB than the Alboran Sea and the Iberian Massif. There is no visible indication in the distribution of the LAB depths of an east-directed subduction from Gibraltar as suggested by tomography. On the contrary, we see shallowing of the LAB to the east below the Alboran Sea. Also, south-directed subduction below the Betics, as suggested by Morales *et al*. (1999), is not supported by our data. There might

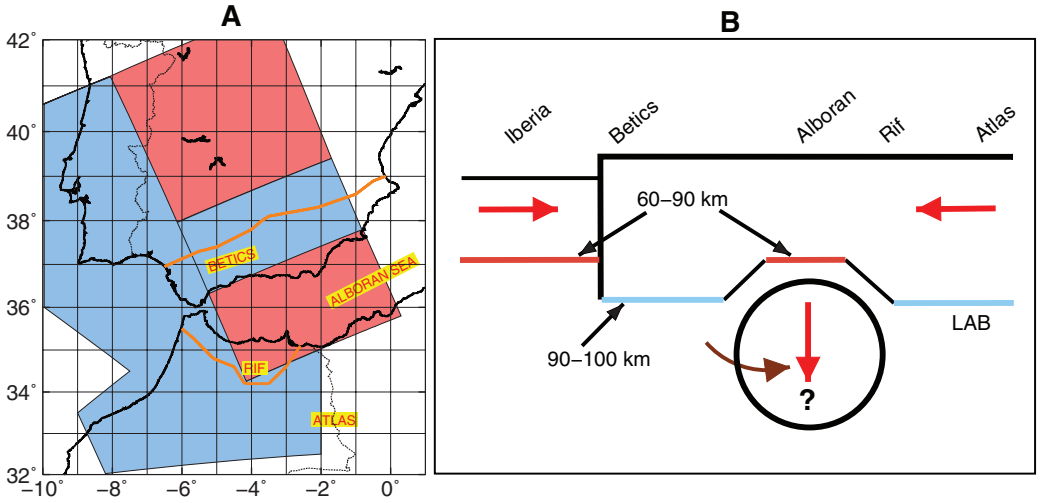

Figure 8. (a) Cartoon of the distribution of LAB depth in the study region; blue areas: 90–100 km depth, red: 60–90 km depth. We chose 90 km as reference depth because there is no LAB depth greater than 90 km in the red regions in (a) and no LAB depth less than 90 km in the blue regions in (a). The Alboran Sea region and large parts of Iberia have a shallow LAB, whereas northwest Africa, the Gibraltar region, southern Portugal and the Betics have a clearly thicker lithosphere. (b) Cartoon showing the interpretation of the data. The observations may be explained by lithospheric delamination in the Alboran Sea region (and possibly in Iberia) of the lower part of the thickened plate. The lithosphere in the eastern Alboran Sea is especially thinned by delamination. Gibraltar and the neighbouring Atlantic seem to remain unaffected by the lithospheric delamination. The rotational arrow indicates a hypothetical explanation for mantle anisotropy observations in the area.

even be some indication of north-directed deepening of the LAB beneath the Betics (see Fig. 4). We think this might be explained by a smooth change from the thinner Alboran lithosphere towards the thicker Betics lithosphere. There are sufficient examples in other parts of the Earth showing that the *S* receiver function technique is able to detect subduction. An example is the Aegean, eastern Mediterranean (Sodoudi *et al*. 2006), where subduction is also obvious from seismicity. Another example is the deep (reaching more than 200 km) continental subduction of India below Tibet, which is not indicated by seismicity (Kumar *et al*. 2006; Kind & Yuan 2010). Therefore, we think that the delamination model (Platt & Vissers 1989; Comas *et al*. 1992; Garcia-Duenas *et al*. 1992; Docherty & Banda 1995; Houseman 1996; Seber *et al*. 1996; Calvert *et al*. 2000) could be able to explain the LAB distribution in the Alboran Sea and surrounding areas. Buontempo *et al*. (2008) and Diaz *et al*. (2010) have interpreted the observed rotation of anisotropy directions, which are parallel to the Betics and the Gibraltar Arc, as being in agreement with the subduction rollback model rather than delamination. They argue that in the delamination model the anisotropy directions should be radial, not tangential. We think there might also be a possibility that a delaminating body might obtain a rotational component in a complicated mantle structure. Fig. 8(b) shows a cartoon of the lithospheric thickness along a north–south cross-section.

Finally, we check the structure of the discontinuities in the upper mantle at 410 and 660 km depth for indications of disturbances due to possible downmoving cold materials. Cold temperature in the mantle transition zone, as expected in a subduction regime, would widen the transition zone (e.g. Helffrich 2000). *P* receiver functions are much more useful to study the 410 and 660 discontinuities than *S* receiver functions because of the conversion angles, which limit the useful distance range for *S* receiver functions. *SKS* receiver functions would be in a more favourable distance range for deep conversions, but they are by far not as numerous as *P* receiver functions. Besides that, shorter period *P* receiver functions result in higher resolution. Fig. 9 shows *P*-to-*S* converted seismic waves at the discontinuities at 410 and 660 km depth. The *P* receiver function traces in two different regions are summed; the Alboran Sea and the closer surroundings (see Fig. 9(a)). The resulting seismic signals are shown in Fig. 9(b). All observed signals of the different regions are in close agreement with each other. There is no hint of local changes in the transition zone thickness. This observation means, in first approximation, that the collisional tectonics of the African and Eurasian plates in the western edge of the Mediterranean does not significantly influence the mantle transition zone. The relatively few deep focus earthquakes in the region are therefore probably caused by relatively small amounts of downward transported materials from the lithosphere.

CONCLUSIONS

We have successfully observed with *S* receiver functions a negative seismic discontinuity (meaning velocity decrease downward) in a large region around the Alboran Sea. This discontinuity is interpreted as the LAB. In recent times, there are many global observations of a negative discontinuity in the upper mantle (e.g. Fischer *et al*. 2010) that is termed LAB, or in cratonic regions, it is also termed mid-lithospheric discontinuity (MLD). There is no general agreement about the interpretation of this discontinuity in cratonic regions. However, there is agreement of the interpretation of this phase as LAB in younger tectonically more active regions (e.g. western United States, see Fischer *et al*. 2010). Therefore, we are confident that the interpretation of our *S* receiver function signals as LAB in the Alboran Sea region is reliable. Also the sharpness of the LAB, which is able to produce converted waves, may be surprising if one considers only a thermal cause for the transition between the lithosphere and asthenosphere. The receiver function observations of a sharper LAB (*S* and *P* receiver functions) indicate that may be additional parameters are involved in forming the global LAB (e.g. partial melt).

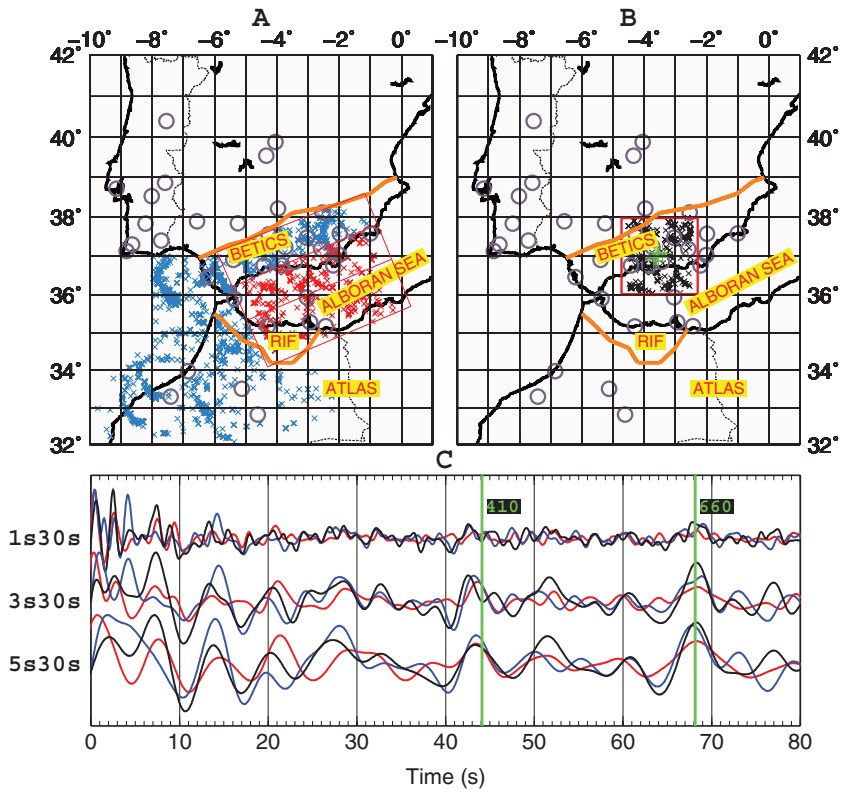

Figure 9. (a) Distribution of piercing points of *P* receiver functions at 520 km depth around the closer Alboran Sea region; red: Alboran Sea, blue: surrounding areas in the Betics and Gulf of Cadiz. (b) Piercing points in the region of very deep earthquakes. (c) Summed *P* receiver functions within the three regions for three different bandpass filters. The theoretical delay times of the discontinuities at 410 and 660 km depth according to the IASP91 global reference model are given by the two green lines. The observed conversions from the two discontinuities agree with each other and also, within about 1 s, with the expected value of the IASP91 model.

Our obtained LAB depth is 90–100 km from the northwest part of Africa to southern Portugal across the Atlantic west of Gibraltar and in the Betics. In the Alboran Sea, the lithosphere thins from 90–100 km near Gibraltar to about 60 km at its eastern end. This observation is in disagreement with models of eastward subduction from Gibraltar beneath the western part of the Alboran Sea. Our results are in better agreement with the delamination model at the Alboran Sea. In a large part of the Iberian Massif, north of the Betics, the LAB is also shallow (70–80 km). This could be in agreement with recent reports on large-scale delamination beneath Iberia (Gutiérrez-Alonso *et al*. 2011).

ACKNOWLEDGMENTS

The data used in this study were provided by the TEDESE-temporary network of UCM, ROA and GEOFON, the Portuguese National Seismic Network, the IAG Network of the Instituto Andaluz de Geofísica and the University of Lisbon Seismic Network. We thank Jose Morales Soto and Flor de Lis Mancilla Pérez from the Instituto Andaluz de Geofísica, Universidad de Granada, for fruitful discussions. We would like to thank two anonymous reviewers for their comments and suggestions on this work. This research was supported by the Deutsche Forschungsgemeinschaft (DFG) and in part by the Ministerio de Ciencia e Innovación (Spain), projects CGL2010–19803-C03–01/02, CSD2006–00041, CGL2008–01830 and P09-RNM-5100. SD was supported by the Friedrich-Ebert Stiftung.

REFERENCES

Ayarza, P., Palomeras, I., Carbonell, A., Afonso, J.C. & Simancas, F., 2010. A Wide-angle upper mantle reflector in SW Iberia, *Phys. Earth planet. Inter.,* **181,** 88–102, doi:10.1016/j.pepi.2010.05.004.

Buforn, E., Coca, P., Udías, A. & Lasa, C., 1997. Source mechanism of intermediate and deep earthquakes in southern Spain, *J. Seismol.,* **1,** 113–130.

Buforn, E., Bezzeghoud, A., Udias, A. & Pto, C., 2004. Seismic sources on the Iberian–African plate boundary and their tectonic implications, *Pure appl. geophys.,* **161,** 623–646, doi:10.1007/s00024-003-2466-1.

Buforn, E., Udias, A., Martin Dávila, J., Hanka, W. & Pazos, A., 2002. Broad band stations network UCM/ROA/GFZ in South Spain and Northern Africa, *Seismol. Res. Lett.,* **73**(2), 183–186.

Buontempo, L., Bokelmann, G.H.R., Barruol, G. & Morales, J., 2008. Seismic anisotropy beneath southern Iberia from SKS splitting, *Earth planet. Sci. Lett.,* **273,** 237–250.

Calvert, A. *et al*., 2000. Geodynamic evolution of the lithosphere and upper mantle beneath the Alboran region of the western Mediterranean: constraints from travel time tomography, *J. geophys. Res.,* **105,** 10 871–10 898.

Carbonell, R. *et al*., 2004. Geophysical evidence of a mantle derived intrusion in SW Iberia, *Geophys. Res. Lett.,* **31,** L11 601–L11 604.

Comas, M.C., Garcia-Duenas, C.V. & Jurado, M.J., 1992. Neogene tectonic evolution of the Alboran Sea from MCS data, *Geo-Mar. Lett.,* **12,** 157–164.

Diaz, J. & Gallart, J., 2009. Crustal structure beneath the Iberian Peninsula and surrounding waters: a new compilation of deep seismic sounding results, *Phys. Earth planet. Inter.,* **173,** 181–190.

Diaz, J. *et al*., 2010. Mantle dynamics beneath the Gibraltar Arc (western Mediterranean) from shear-wave splitting measurements on a dense seismic array, *Geophys. Res. Lett.,* **37,** L18304, doi:10.1029/2010GL044201.

Docherty, C. & Banda, E., 1995. Evidence for the eastward migration of the Alboran Sea based on regional subsidence analysis: a case for basin formation by delamination of the subcrustal lithosphere, *Tectonics,* **14,** 804–818.

Ducea, M.H., 2011. Fingerprinting orogenic delamination, *Geology,* **39,** 191–192, doi:10.1130/focus022011.1.

Fadil, A. *et al*., 2006. Active tectonics of the Western Mediterranean: GPS evidence for roll back of a delaminated subcontinental slab beneath the Rif Mountains, Morocco, *Geology,* **34,** 529–532, doi:10.1130/G22291.1.

Fischer, K.M., Ford, H.A., Abt, D.L. & Rychert, C.A., 2010. The lithosphere-asthenosphere boundary, *Annu. Rev. Earth planet. Sci.,* **38,** 551–575, doi:10.1146/annurev-earth-040809-152438.

Fullea, J., Fernàndez, M., Zeyen, H., & Vergés, J., 2007. A rapid method to map the crustal and lithospheric thickness using elevation, geoid anomaly and thermal analysis. Application to the Gibraltar Arc System and adjacent zones. *Tectonophysics,* **430**(1–4), 97–117.

Fullea, J., Afonso, J.C., Connolly, J.A.D., Fernández, M., Garcia-Castellanos, D. & Zeyen, H. 2009. LitMod3D: an interactive 3-D software to model the thermal, compositional, density, seismological, and rheological structure of the lithosphere and sublithospheric upper mantle, *Geochem. Geophys. Geosyst.,* **10,** doi:10.1029/2009GC002391.

Garcia-Duenas, V., Balanya, J.C. & Martinez-Martinez, J.M., 1992. Miocene extensional detachments in the outcropping basement of the northern Alboran basin (Betics) and their tectonic implications, *Geo-Mar. Lett.,* **12,** 88–95.

Gutiérrez-Alonso, G., Murphy, J.B., Fernández-Suárez, J., Weil, A.B., Franco, M.P. & Gonzalo, J.C., 2011. Lithospheric delamination in the core of Pangea: Sm-Nd insights from the Iberian mantle. *Geology,* **39,** 155–158, doi: 10.1130/G31468.1.

Gutscher, M.-A., Malod, J., Rehault, J.-P., Contrucci, I., Klingelhoefer, L., Mendes-Victor, L. & Spakman, W., 2002. Evidence for active subduction beneath Gibraltar, *Geology,* **30**(12), 1071–1074.

Helffrich, G., 2000. Topography of the transition zone seismic discontinuities, *Rev. Geophys.,* **38,** 141–158.

Houseman, G., 1996. From mountains to basin, *Nature,* **379,** 771–772.

Kennett, B.L.N. & Engdahl, E.R., 1991. Traveltimes for global earthquake location and phase identification, *Geophys. J. Int.,* **105,** 429–465, doi:10.1111/j.1365-246X.1991.tb06724.x.

Kind, R. & Yuan, X.H., 2010. Seismic images of the biggest crash on Earth, *Science,* **329,** 1479–1480.

Kumar, P., Yuan, X.H., Kind, R. & Ni, J., 2006. Imaging the colliding Indian and Asian lithospheric plates beneath Tibet, *J. geophys. Res.,* **111,** B06308, doi:10.1029/2005JB003930.

Lonergan, L. & White, N., 1997. Origin of the Betic-Rif mountain belt, *Tectonics,* **16,** 504–522.

Martinez-Solares & López Arroyo, 2004. The great historical 1755 earthquake: effects and damage in Spain, *J. Seismol.,* **8,** 275–294.

Martinez, M.D., Lana, X., Caselles, O., Canas, J. A. & Pujades, L., 2005. Elastic-anelastic regional structures for the Iberian peninsula obtained from Rayleigh wave tomography and causal uncoupled inversion, *Pure appl. Geophys.,* **162,** 2321–2353, doi:10.1007/s00024-005-2778-4.

McClusky, S., Reilinger, R., Mahmoud, S., Ben Sari, D. & Tealeb, A., 2003. GPS constraints on Africa (Nubia) and Arabia plate motions, *Geophys. J. Int.,* **155,** 126–138.

Michard, A., Chalouan, A., Feinberg, H., Goffé, B. & Montigny, R., 2002. How does the Alpine belt end between Spain and Morocco? *Bull. Soc. Geol. France,* **173,** 3–15.

Morales, J., Serrano, I., Jabaloy, A., Galindo-Zaldivar, J., Zhao, D., Torcal, F., Vidal, F. & Gonzalez-Lodeiro, F., 1999. Active continental subduction beneath the Betic Cordillera and the Alboran Sea, *Geology,* **27,** 735–738.

Morley, C.K., 1993. Discussion of the origins of hinterland basins to the Rif-Betic cordillera and Carpathians, *Tectonophysics,* **226,** 359–376.

Muñoz, D. & Udías, A., 1988. Evaluation of damage and source parameters of the Málaga earthquake of 9 October 1680, in *Historical Seismograms and Earthquakes of the World,* pp. 208–221, eds Lee,W.H.K., Meyer H. & Shimazaki K., Academic Press, San Diego.

Palomeras, I., Carbonell, R., Ayarza, P., Fernández, M., Simancas, J.F., Martínez Poyatos, D., González Lodeiro, F. & Pérez-Estaún, A., 2010. Geophysical model of the lithosphere across the Variscan Belt of SW-Iberia: multidisciplinary assessment, *Tectonophysics,* **508,** doi:10.1016/j.tecto.2010.07.010.

Perouse, E., Vernant, P., Chery, J., Reilinger, R. & McClusky, S., 2010. Active surface deformation and sub-lithospheric processes in the western Mediterranean constrained by numerical models, *Geology,* **38,** 823–826, doi:10.1130/G30963.1.

Platt, J. & Vissers, R., 1989. Extensional collapse of thickened continental lithosphere: a working hypothesis for the Alboran Sea and Gibraltar arc, *Geology,* **17,** 540–543.

Royden, L.H., 1993. Evolution of retreating subduction boundaries formed during continental collision, *Tectonics,* **12,** 629–638.

Sandvol, E., Seber, D., Calvert, A. & Barazangi, M., 1998, Grid search modeling of receiver functions: implications for the crustal structure in the Middle East and in North Africa, *J. geophys. Res.,* **103,** 26 899–26 917.

Seber, D., Barazangi, M., Ibenbrahim, A. & Demnati, A., 1996. Geophysical evidence for lithospheric delamination beneath the Alboran Sea and Rif–Betic mountains, *Nature,* **379,** 785–790.

Simancas, F. *et al*., 2003. Crustal structure of the transpressional Variscan orogen of SW Iberia: SW Iberia deep seismic reflection profile (IBERSEIS), *Tectonics,* **22**(6), 1062.

Sodoudi, F. *et al*., 2006. Lithospheric structure of the Aegean obtained from P and S receiver functions, *J. geophys. Res.,* **111,** B12307.

Spakman, W. & Wortel, R., 2004. A tomographic view on Western Mediterranean Geodynamics, in *The TRANSMED Atlas, The Mediterranean Region from Crust to Mantle,* pp. 31–52, eds Cavazza, W., Roure, E.M., Spakman, W., Stampfli, G.M. & Ziegler, P., Springer-Verlag, Berlin.

Vernant, P., *et al*., 2010. Geodetic constraints on active tectonics of the, Western Mediterranean: implications for the kinematics and dynamics of the Nubia-Eurasia plate boundary zone, *J. Geodyn.,* **49,** 123–129.

Wigger, P., Asch, G., Giese, P., Heinsohn, W.D., El Alami, S.O. & Ramdani, F., 1992. Crustal structure along a traverse across the Middle and High Atlas mountains derived from seismic refraction studies, *Geologische Rundschau,* **81,** 237–248.

Yuan, X., Kind, R., Li, X. & Wang, R., 2006. S receiver functions: synthetics and data example, *Geophys. J. Int.,* **175**(2), 555–564.

Zitellini, N. *et al*., 2009. The quest for the Africa–Eurasia plate boundary west of the Strait of Gibraltar, *Earth planet. Sci. Lett.,* **280**(1–4), 13–50.